



## ORIGINAL ARTICLE

# Rheological behavior, hydration, and mechanical properties of LC<sup>3</sup> systems with the incorporation of functionalized multi-walled carbon nanotubes

*Comportamento reológico, hidratação e propriedades mecânicas de sistemas LC<sup>3</sup> com a incorporação de nanotubos de carbono de paredes múltiplas funcionalizados*

Laura Silvestro<sup>a</sup>

Artur Spat Ruviano<sup>b</sup>

Francisco Roger Carneiro Ribeiro<sup>c</sup>

Philippe Jean Paul Gleize<sup>b</sup>

Ana Paula Kirchheim<sup>c</sup>

<sup>a</sup>Universidade Tecnológica Federal do Paraná – UTFPR, Guarapuava, PR, Brasil

<sup>b</sup>Universidade Federal de Santa Catarina – UFSC, Laboratory of Application of Nanotechnology in Civil Construction, Florianópolis, SC, Brasil

<sup>c</sup>Universidade Federal do Rio Grande do Sul – UFRGS, Laboratory of Innovation in Eco-Efficient Cements, Porto Alegre, RS, Brasil

Received 11 January 2023

Revised 17 March 2023

Accepted 04 April 2023

Corrected 27 March 2024

**Abstract:** Alternatives to conventional Portland cement with a more sustainable appeal are increasingly recurrent. Among these are the Limestone Calcined Clay (LC<sup>3</sup>) systems, characterized by high replacement percentages of Portland clinker by calcined clay and limestone, materials widely available worldwide. A complete understanding of the rheological behavior of LC<sup>3</sup> systems is necessary for the practical application of this type of cement to be consolidated. Furthermore, although not yet investigated, the incorporation of nanomaterials stands out as a promising alternative for accelerating reactions and enhancing the mechanical performance of these systems at early ages. This study investigated the incorporation of carbon nanotubes (CNT) contents from 0.05 to 0.125% in an LC<sup>3</sup> system through rotational rheometry, isothermal calorimetry, compressive strength at 7 and 28 days, and X-ray diffraction. Although the CNT incorporation increased the dynamic yield stress and equivalent viscosity of the LC<sup>3</sup> pastes, the content of 0.1 wt.% slightly increased and anticipated the occurrence of the main peak of the aluminates. Increases of up to 13.5% in compressive strength at 7 and 28 days of hydration were observed for a CNT content of 0.1 wt.%.

**Keywords:** LC<sup>3</sup>, carbon nanotubes, composites, rheology, hydration.

**Resumo:** Alternativas ao cimento Portland convencional com apelo mais sustentável são cada vez mais recorrentes. Entre elas estão os sistemas *Limestone Calcined Clay* (LC<sup>3</sup>), caracterizados por altos percentuais de substituição do clínquer Portland por argila calcinada e calcário, materiais amplamente disponíveis em todo o mundo. Um completo entendimento do comportamento reológico dos sistemas LC<sup>3</sup> é necessário para que a aplicação prática deste tipo de cimento seja consolidada. Além disso, embora ainda não investigada, a incorporação de nanomateriais se destaca como uma alternativa promissora para acelerar reações e melhorar o desempenho mecânico desses sistemas em idades precoces. Este estudo investigou a incorporação de teores de nanotubos de carbono (CNT) de 0,05 a 0,125% em um sistema LC<sup>3</sup> por meio de reometria rotacional, calorimetria isotérmica, resistência à compressão aos 7 e 28 dias e difração de raios-X. Embora a incorporação de CNT tenha aumentado a tensão de escoamento e a viscosidade equivalente das pastas LC<sup>3</sup>, o teor de 0,1% aumentou ligeiramente e antecipou a ocorrência do pico principal dos aluminatos. Aumentos de até 13,5% na resistência à compressão aos 7 e 28 dias de hidratação foram observados para um teor de CNT de 0,1% em massa.

**Palavras-chave:** LC<sup>3</sup>, nanotubos de carbono, compósitos, reologia, hidratação.

**Corresponding author:** Laura Silvestro. E-mail: laurasilvestro@utfpr.edu.br

**Financial support:** None.

**Conflict of interest:** Nothing to declare.

**Data Availability:** the data that support the findings of this study are openly available in Scielo Data at <https://doi.org/10.48331/scielodata.YB6XVR>.

This document has an erratum: <https://doi.org/10.1590/S1983-41952024000100011>



This is an Open Access article distributed under the terms of the Creative Commons Attribution License, which permits unrestricted use, distribution, and reproduction in any medium, provided the original work is properly cited.

**How to cite:** L. Silvestro, A. S. Ruviaro, F. R. C. Ribeiro, P. J. P. Gleize, & A. P. Kirchheim, "Rheological behavior, hydration, and mechanical properties of LC<sup>3</sup> systems with the incorporation of functionalized multi-walled carbon nanotubes," *Rev. IBRACON Estrut. Mater.*, vol. 17, no. 1, e17106, 2024, <https://doi.org/10.1590/S1983-41952024000100006>

## 1 INTRODUCTION

The Portland cement production chain emits up to 9.0% of the total carbon dioxide (CO<sub>2</sub>) released worldwide [1]. This sector has made several efforts to reduce this environmental impact, such as lowering the clinker factor through supplementary cementitious materials (SCM) [1], [2]. However, new alternatives must be considered, given the global trend towards implementing zero-carbon emission policies [3]. Several countries have committed to the Climate Ambition Alliance to achieve net-zero CO<sub>2</sub> emissions by 2050 [4]. According to Rissman et al. [5], net-zero greenhouse gas emissions must be reached by 2050-2070 to limit global warming to 2 °C. Thus, new alternative materials to Portland cement (PC) with a lower CO<sub>2</sub> emission need to be studied and developed. Within this framework, limestone calcined clay cement, denominated LC<sup>3</sup>, has been extensively researched and stands out as a promising alternative to reduce the environmental impact of the PC production sector [6], [7]. Previous studies indicated that LC<sup>3</sup> systems could reduce CO<sub>2</sub> emissions compared to PC by up to 40% [6] and 60% [8].

LC<sup>3</sup> systems are composed of PC, calcined clay, and limestone. These systems are characterized by a synergistic effect between the calcined clay and limestone that forms carboaluminates phases, which allows clinker replacement percentages higher than those usually adopted for SCM [6], [7]. Although the LC<sup>3</sup> systems have high percentages of clinker replacement (in the order of 50 wt.%), they have a similar mechanical performance to PC after 7 days of hydration [9]. Additionally, although the use of SCM contributes to reducing carbon emissions and consuming resources in cement production, the availability of these materials in several regions is a limiting factor for their use on a large scale. Slag production represents 5 to 10% of the current cement demand worldwide. Similarly, fly ash represents approximately 30% of this demand. Considering this problem, clays are widely available worldwide, representing a great advantage of the LC<sup>3</sup> system [10]. Estimates indicate that clay and limestone reserves can supply the current and growing demand for cement for more than 1 million years [11], [12]. High-purity kaolinitic clays are widely used to produce metakaolin, producing a high-reactivity material [13].

The high specific surface area of most clays used in these systems and the large reduction in the clinker factor can negatively affect the fresh state of LC<sup>3</sup> systems. Hence, one of the main factors that affect the practical application of LC<sup>3</sup> is related to their rheological behaviour. Thus, understanding the rheological properties of LC<sup>3</sup> cement becomes fundamental for this type of material's wide application and use [14]. Nevertheless, according to Ferreira et al. [15], few studies addressed the undesirable rheological properties characteristic of LC<sup>3</sup> systems.

The incorporation of materials such as nano-silica, carbon nanotubes (CNT), and C-S-H nanoparticles [16] are being studied to improve the properties of cement-based materials. CNT have been widely applied due to their excellent thermal, electrical, and mechanical properties [17]–[21]. The CNT incorporation in PC matrices to increase mechanical properties and durability is already well established. Overall, research indicates that adding small amounts of CNT (on the order of 0.1% by cement weight) increases cementitious composites' compressive and flexural strengths by up to 30% and 50%, respectively [22]. This behavior can be attributed to the CNT nucleation effect [23] and the reduction of the total porosity and the size of the pores of the cementitious matrix [24]. Furthermore, CNT acts by connecting and restricting the propagation of cracks, improving the mechanical properties of cementitious composites [25].

Previous studies evaluated the incorporation of CNT and nano-clays (NC) in cement-based materials. For instance, Gamal et al. [26] observed that the combined incorporation of CNT-NC enhanced concretes' mechanical performance and durability properties, with increases of up to 26.4% in 28-d compressive strength. Similarly, Morsy et al. [27] also reported that the 28-d compressive strength of mortar composed of 6.0 wt.% of NC and 0.02 wt.% of CNT was 29.0% higher than the plain mortar. Ma et al. [28] assessed mortars' rheological and hardened properties with CNT and palygorskite clays. The authors observed that combining both materials significantly increased the yield stress and the 28-d compressive strength compared to the control mortar. Additionally, previous studies have indicated that incorporating SCM (e.g., silica fume) can improve the CNT dispersion in cementitious matrices due to the smaller particle size of these materials and, consequently, enhance the mechanical performance of composites [25], [29].

It is noteworthy that the LC<sup>3</sup> systems are characterized by lower compressive strength at early ages, considering that the pozzolanic activity of calcined clays occurs at later ages (> 7 days), and the formation of the carboaluminates phases starts only after 1 day of hydration [30]–[32]. In this context, Lin et al. [29] identified that nano-silica could enhance the low early-age strength and carbonation resistance of LC<sup>3</sup> concretes. Nevertheless, the CNT incorporation in LC<sup>3</sup> systems has not yet been investigated. Thus, the addition of CNT in LC<sup>3</sup> systems has great potential to increase the mechanical performance and reduce the porosity of composites, mainly at an early age. This research aimed to investigate the effect of CNT incorporation on the rheological parameters, hydration kinetics, and compressive strength of LC<sup>3</sup> systems.

## 2 MATERIALS AND METHODS

### 2.1 Materials

A Portland clinker was used to produce the LC<sup>3</sup> systems. Its mineralogical composition, presented in Table 1 was determined by X-ray diffraction (XRD) through quantitative Rietveld analysis. The test was carried out using an X'Pert Pro (PANalytical) diffractometer, operating with the following parameters: 45 kV, 40 mA, CuK $\alpha$  radiation ( $\lambda = 1.5418 \text{ \AA}$ ), scanning range of 7–70 $^{\circ}$  2 $\theta$ , and step size of 0.0167 2 $\theta$ . Rietveld analysis was performed on TOPAS v5 using the ICSD database.

**Table 1.** Mineralogical composition of Portland clinker.

Phase	PC (wt. %)
C <sub>3</sub> S M3	62.86
C <sub>2</sub> S $\beta$	16.29
C <sub>3</sub> A cub	7.08
C <sub>4</sub> AF	8.43
Periclase	1.94
Aphthitalite	1.06
Portlandite	2.35
Rwp (%)	6.40

Pure gypsum (99.16 wt. % CaSO<sub>4</sub>·2H<sub>2</sub>O) was used as a calcium sulfate source, and calcitic limestone (Figure S1 <https://doi.org/10.48331/scielodata.YB6XVR>) was employed for LC<sup>3</sup> production. One can note that the limestone filler was not heat treated. Moreover, commercial kaolin was purchased to produce metakaolin. Initially, a study of the optimal thermal activation temperature of the material was conducted. The kaolin was treated heat in a muffle (KK260, Linn Elektro Therm GmbH) for 2 h at different temperatures (600, 700, 800, and 900  $^{\circ}$ C). Figure S2 (<https://doi.org/10.48331/scielodata.YB6XVR>) shows the XRD patterns in natura kaolin and metakaolin (MK) after heat treatment at different temperatures. The main crystalline phases identified were kaolinite and quartz. For a thermal activation temperature of 600  $^{\circ}$ C, kaolinite peaks were still identified (e.g., 12.3 $^{\circ}$  and 24.7 $^{\circ}$  2 $\theta$ ). Nevertheless, for temperatures above 700  $^{\circ}$ C, the absence of reflections peaks assigned to kaolinite was observed, indicating its complete dehydroxylation and the consequent formation of metakaolin. Furthermore, from increasing the temperature to 700  $^{\circ}$ C onwards, no expressive changes were observed in the diffractograms, suggesting that the optimal temperature was 700  $^{\circ}$ C. The limestone, kaolin, and metakaolin diffractograms were obtained with the equipment and conditions described in Section 2.3.

The R<sup>3</sup> test (Rapid, Relevant, and Reliable) developed by Avet et al. [9] also evaluated the kaolin's optimal calcination temperature. Therefore, the binary systems methodology was adopted, and the total cumulative heat for 144 h at 20  $^{\circ}$ C (equipment described in section 2.3) was evaluated. Figure S3 (<https://doi.org/10.48331/scielodata.YB6XVR>) shows the results of the R<sup>3</sup> test for in natura and calcined kaolin at temperatures of 600, 700, 800, and 900  $^{\circ}$ C. The results showed that a calcination temperature of 700  $^{\circ}$ C produced the highest cumulative heat. Thus, the R<sup>3</sup> test also indicated that the kaolin optimal calcination temperature was 700  $^{\circ}$ C, corroborating with the XRD results previously discussed.

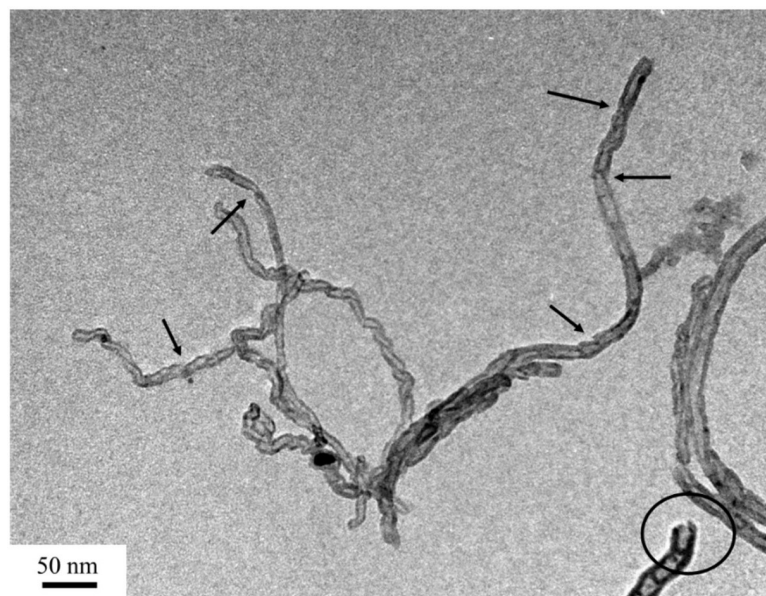
Figure S4 (<https://doi.org/10.48331/scielodata.YB6XVR>) shows the zeta potential of kaolin and metakaolin after heat treatment at different temperatures. The test was performed on a Malvern Zetasizer Nano. Dispersions of deionized water and kaolin/metakaolin with a concentration of 0.2 wt.% were evaluated. The kaolin exhibited a zeta potential of – 10.5 mV, in agreement with the values reported by Sposito et al. [33] for common clays. The negative values can be attributed to the charge of the basal faces of the clay materials [34]. Moreover, metakaolin's absolute zeta potential values increased with the calcination, reaching higher values for higher temperatures ( $\geq 700 \text{ }^{\circ}\text{C}$ ). Sposito et al. [33] also found that the absolute zeta potential values of calcined clays increase with higher calcined kaolinite contents, corroborating the results obtained in this study. The zeta potential results were in line with the XRD and R<sup>3</sup> tests previously discussed.

The chemical composition and physical properties of Portland clinker, MK (calcined at 700  $^{\circ}$ C), and limestone (LS) are shown in Table 2. The chemical composition was assessed by X-ray fluorescence (Epsilon 1, Panalytical). The particle size distribution was evaluated using a Particle Size Analyzer S3500 (Microtrac). The specific surface area was determined using an Autosorb (Quantachrome Instruments) applying the Brunauer–Emmett–Teller (BET) procedure.

**Table 2.** Chemical composition and physical properties of Portland clinker, MK, and LS.

Property	Clinker	MK	LS
<i>Chemical composition (wt.%)</i>			
SiO <sub>2</sub>	15.77	52.25	1.91
Al <sub>2</sub> O <sub>3</sub>	4.38	44.98	0.78
Fe <sub>2</sub> O <sub>3</sub>	3.59	0.44	0.63
CaO	68.63	0.09	53.01
MgO	1.75	-	2.40
SO <sub>3</sub>	1.47	-	0.06
Na <sub>2</sub> O	-	-	-
K <sub>2</sub> O	1.210	0.70	0.08
Loss on ignition	3.200	1.54	41.13
<i>Physical property</i>			
D <sub>10</sub> (μm)	2.49	2.21	2.93
D <sub>50</sub> (μm)	9.95	3.29	10.72
D <sub>90</sub> (μm)	30.24	7.46	35.16
Mean diameter (μm)	13.97	5.04	15.94
Density (g/cm <sup>3</sup> )	3.23	2.51	2.75
B.E.T. Specific surface area (m <sup>2</sup> /g)	2.56	9.30	1.29

A polycarboxylate-based (PCE) superplasticizer admixture (Tec-flow 8000, GCP Applied Technologies) was employed for LC<sup>3</sup> paste production. Multi-walled carbon nanotubes (CNT) functionalized with the carboxyl group were used. The CNT supplied by Nanostructured & Amorphous Materials Inc had a carboxyl content of 1.9–2.1%, purity >95%, an inner diameter of 5–10 nm, an outer diameter of 20–30 nm, length of 10–30 μm, and specific surface area >200 m<sup>2</sup>/g. Figure 1 shows a transmission electron microscopy of the CNT acquired using a JEM-1011 (Joel). As observed, the CNT's diameter follows the intervals informed by the manufacturer. Furthermore, the treatment for the oxidation of CNT (i.e., insertion of carboxyl groups), usually conducted through acid treatment, caused some defects on the nanomaterial's surface, as can be seen by the arrows in Figure 1 that indicated the cavities in the tubular structure of the CNT [35]. Moreover, the end tips of CNT are opened, as pointed out by the circle in Figure 1, which indicates that the oxidation treatment broke C-C bonds, allowing the generation of functional groups in these regions [36].

**Figure 1.** TEM image of CNT (at ×600,000 magnification).

## 2.2 Mixture design

LC<sup>3</sup> systems composed of 50% clinker Portland, 30% metakaolin, 15% limestone filler, and 5% calcium sulfate [2] were evaluated, as presented in Table 3. The cement pastes were produced with a water-to-binder (w/b) ratio of 0.6. This value was adopted based on previous studies by the research group [30], [37], which identified that LC<sup>3</sup> systems usually need more water, mainly considering the properties in the fresh state. CNT contents between 0.05% and 0.125% by cement weight were evaluated. These values were determined based on the contents used in PC matrices [22]. A fixed PCE content was added in all compositions, including in the reference (REF). The PCE was added to improve the flowability of LC<sup>3</sup> systems and to aid in the dispersion of CNT. This approach of keeping the SP content fixed aimed to evaluate the isolated effect of the CNT incorporation. Initially, the CNT and PCE were added to the water and dispersed via sonication using a probe sonication Vibra-Cell with a diameter of 13 mm (VCX Serie, 750 W, 20 kHz) operating at an amplitude of 50% for 6 min [38]–[40]. This dispersion process was conducted in an ice bath to prevent the overheating of CNT aqueous dispersions. Subsequently, the CNT aqueous dispersions were added to the anhydrous materials (previously homogenized) and mixed manually for 30 s and, after 20 s of rest, mechanically mixed for 70 s in a high-shear mixer (10,000 rpm).

**Table 3.** Detailed composition of LC<sup>3</sup> cementitious composites.

Cement paste	Clinker (g)	MK (g)	LS (g)	Calcium sulfate (g)	Water (g)	PCE (g)	CNT (g)	Energy (J)	Mini slump (mm)
REF	50.0	30.0	15.0	5.0	60.0	0.25	-	-	87
0.05CNT	50.0	30.0	15.0	5.0	60.0	0.25	0.050	11,636	75
0.075CNT	50.0	30.0	15.0	5.0	60.0	0.25	0.075	12,064	71
0.1CNT	50.0	30.0	15.0	5.0	60.0	0.25	0.100	12,854	69
0.125CNT	50.0	30.0	15.0	5.0	60.0	0.25	0.125	13,467	71

## 2.3 Experimental methods

The rheological behaviour of CNT cementitious composites was assessed through rotational rheometry. The tests were conducted using a Haake MARS III (Thermo Fisher Scientific) rheometer with a hatched parallel-plate geometry with a diameter of 35 mm and a gap of 1.000 mm. A pre-shear of 100 s<sup>-1</sup> was initially applied during the 60s to homogenize the samples. Subsequently, after a rest period of 60s, the ascending flow curve (shear stress vs shear rate) was determined by increasing the shear rate from 0.1 to 100 s<sup>-1</sup> in: (i) 4 steps distributed logarithmically between 0.1 and 10 s<sup>-1</sup> and (ii) 6 steps distributed linearly from 25 to 100 s<sup>-1</sup>. The descending flow curve was obtained following the same routine described for the ascending curve. In each step, the shear rate was applied for 10 s and only the last 3 seconds were recorded, ensuring stabilization of the shear stress measurement [41]. The dynamic yield stress of the cement pastes evaluated was obtained by applying the Herschel-Bulkley (H-B) model (Equation 1) to the descending flow curve. The equivalent plastic viscosity was calculated using the equation proposed by De Larrard (Equation 2) [42]. The rotational rheometry was conducted for 60 min with measurements every 10 minutes. An insulation chamber was used to prevent the loss of water from the samples.

$$\tau = \tau_0 + K \cdot \dot{\gamma}^n \quad (1)$$

$$\mu_{eq} = \frac{3K}{n+2} \cdot (\dot{\gamma}_{max})^{n-1} \quad (2)$$

Where  $\tau$  is the shear stress (Pa),  $\tau_0$  is the dynamic yield stress,  $K$  and  $n$  are, respectively, the consistency and the pseudoplastic parameters of the H-B model,  $\dot{\gamma}$  is the shear rate (s<sup>-1</sup>),  $\dot{\gamma}_{max}$  is the maximum shear rate applied (100 s<sup>-1</sup>), and  $\mu_{eq}$  is the equivalent plastic viscosity.

A good fit of all samples was obtained through H-B ( $R^2 > 0.9987$ ). Furthermore, all cement pastes evaluated showed  $n$  values between 0.576 and 0.753, indicating a shear-thinning response. Thus, a linear fit such as that of the Bingham model would be inadequate to describe the rheological behaviour of the pastes.

Initially, the rotational rheometry test was conducted on two independent fresh samples of REF cement paste to determine the variability of the test. The measurements performed in duplicate showed average variations of 5.2% and 6.0% for dynamic yield stress and equivalent viscosity values, respectively. Thus, these average variations were considered to estimate the standard deviation of the other evaluated compositions. Moreover, the fluidity of CNT cement composites was assessed through the mini-slump test [43].

The initial hydration of the LC<sup>3</sup> systems with the incorporation of CNT was evaluated through isothermal calorimetry. The test was performed on a TAM Air (TA Instruments) calorimeter, keeping the temperature at 23 °C. The cement pastes were produced following the same procedure described in section 2.2. Subsequently, samples with approximately 10 g were added to the vials for the test, which was conducted for 120 h. The mass of anhydrous materials normalized the heat flow and cumulative heat values. Furthermore, the first 60 minutes of measurement were disregarded to determine the cumulative heat of the samples.

The compressive strength of the cement pastes was evaluated after 7 and 28 days of hydration. Six cylindrical samples with a diameter of 20 mm and a height of 26 mm were molded for each composition and evaluated age. The mean value of the samples was adopted as the compressive strength values. The analysis of variance (ANOVA) of the results was performed in the Origin software, assuming a significance level of 0.05.

XRD of CNT cementitious composites after 7 and 28 days of hydration was conducted on a Miniflex II Desktop X-Ray Diffractometer (Rigaku) with CuK radiation ( $\lambda = 1.5418 \text{ \AA}$ ), operating at 30 kV/15 mA. The test was carried out from 7° to 55° (2 $\theta$ ) with a 0.03° 2 $\theta$  step size. The cement hydration of the samples was stopped with the solvent exchange using isopropanol. After that, the samples were ground, sifted in a 45  $\mu\text{m}$ -opening mesh, and kept in a desiccator. The crystalline phase identification was conducted on Match! Software using the COD (Crystallography Open Database)

### 3. RESULTS AND DISCUSSION

#### 3.1 Rheological behaviour

Figure 2 exhibits the flow and viscosity curves of the plain cement paste (REF) during the first 60 minutes of hydration to exemplify the rheological behaviour of LC<sup>3</sup> systems. The systems showed significant increases in the values of shear stress and viscosity between the measurements performed at 10 min and 20 min, with progressive growth of both values over time. These fresh state properties of LC<sup>3</sup> systems can be attributed to the MK characteristic such as high negative zeta potential (-31.3 mV – see Figure S4) and high specific surface area (~263% higher than clinker), which increase the flocculation of the systems [33], [44], [45]. According to Sposito et al. [33], the higher the zeta potential, the higher the resistance to flow and water demand of LC<sup>3</sup> systems. The PCE can also intercalate into the MK structure, reducing efficiency [15]. Besides that, the negative surface of MK can adsorb significant amounts of Ca<sup>2+</sup> ions, turning its surface positive and thus increasing the uptake of PCE of the system, whereas the PCE is usually adsorbed onto positive charge surfaces [34].

Furthermore, the calcined clays (e.g., MK), usually characterized by a high reactivity, can exhibit a strong initial ettringite formation in LC<sup>3</sup> systems [33]. Thus, the time-dependent fresh-state properties are also influenced by ettringite formation [46]. Another aspect that should be considered is that MK has a lower density compared to PC, which results in a greater volume of material since the replacement of PC by MK was conducted by weight. According to Navarrete et al. [47], the effect of supplementary cementitious materials on the viscosity of cementitious materials is better explained by the particle number density and solid volume fraction than by the specific surface area of the particles.

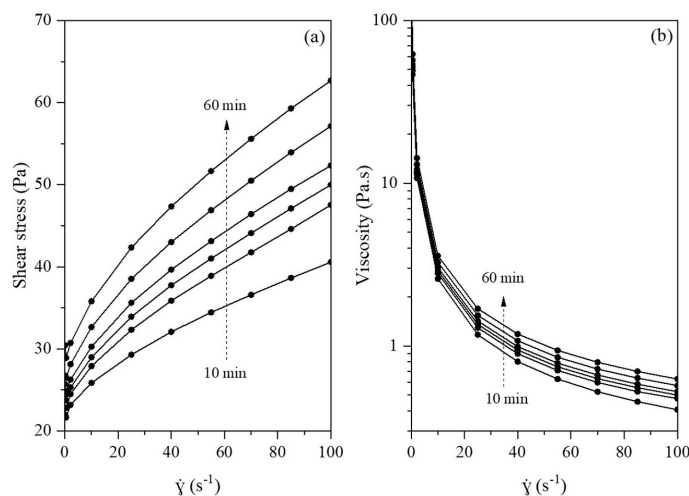


**Figure 2.** Rheological behavior of REF cement pastes over time: (a) flow curves and (b) viscosity vs. shear rate.

The rheological parameters of CNT composites are shown in Figure 3. Increases in the dynamic yield stress and equivalent viscosity of 30.5% and 85.0% were observed from 10 to 60 min for the plain cement paste, respectively. The same trend was observed for CNT-LC<sup>3</sup> composites. For instance, yield stress and viscosity growth were 16.4% and 51.5%, respectively, for the LC<sup>3</sup> system with the addition of 0.125 wt.% of CNT. These results indicate that the hydration time has a more pronounced impact on the viscosity of LC<sup>3</sup> systems, i.e., on the resistance to flow after the yield stress is overcome, than on the dynamic yield stress required for the material to flow. Thus, the yield stress can be associated with a cement-based material's filling capacity and the possibility of the material flowing under applied stress. In contrast, the viscosity is related to the flow velocity when initiated [48]. The viscosity can affect several practical applications, such as pumping and casting rates [49].

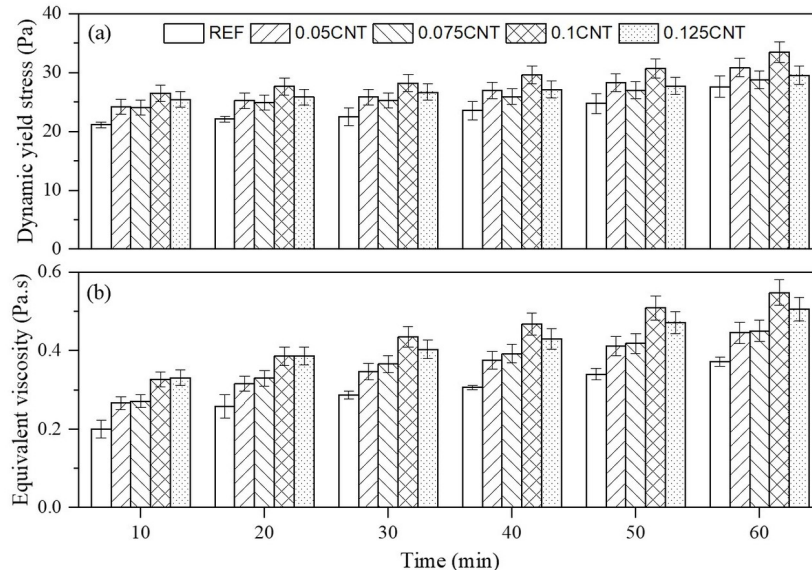


**Figure 3.** Rheological parameters of CNT cementitious composites over time: (a) dynamic yield stress and (b) equivalent viscosity. Error bars correspond to  $\pm 1$  estimated standard deviation.

The CNT incorporation overall progressively increased the systems' dynamic yield stress and equivalent viscosity. For instance, at 10 min, the increases in yield stress were of 14.3% (0.05CNT), 13.6% (0.075CNT), 25.5% (0.1CNT), and 20.2% (0.125CNT) compared to the plain cement paste (i.e., REF). These values were 30.0% (0.05CNT), 35.0% (0.075CNT), 60.0% (0.1CNT), and 65.0% (0.125CNT) for the equivalent viscosity after 10 minutes of hydration. A similar trend was observed for the other measurement times (20–60 min). These results follow the incorporation of CNT in Portland cementitious composites. Jiang et al. [50] observed that adding 0.1 wt.% of CNT increased the yield stress and plastic viscosity by around 169.0% and 532.0%, respectively, compared to the control cement paste. Reales et al. [51] reported increases in the yield stress of cement pastes of approximately 16.0% and 200.0% for CNT contents of 0.05 wt.% and 0.1 wt.%, respectively, compared to plain cement paste. Moreover, while adding 0.05 wt.% of CNT did not affect the plastic viscosity of the cement paste, the incorporation of 0.15 wt.% of CNT resulted in an increase of 266.0% for this rheological parameter [51]. Silvestro et al. [40] observed that a carboxyl-functionalized CNT content of 0.1 wt.% increased the dynamic yield stress and equivalent viscosity of PC cement pastes ( $w/c = 0.4$ ) by 98.0% and 127.0%, respectively. Similar to the influence of hydration time on the rheological parameters, the CNT incorporation also exhibited a more pronounced effect on the equivalent viscosity than on the dynamic yield stress of the LC<sup>3</sup> systems. Thus, considering that the yield stress is related to the intergranular friction among the particles and the viscosity is associated with the water flow in the porosity of granular systems [52], the results indicate that CNT incorporation affects the water demand of the compositions [53]. This trend possibly is related to the specific surface area of CNT, as previously mentioned, and the presence of hydrophilic groups on the CNT's surface (i.e., carboxyl groups), which can adsorb the water from the mixture [54], [55].

Nevertheless, it seems that the CNT incorporation has a lower negative impact on the fresh properties of LC<sup>3</sup> systems than on the Portland cement matrices (compared to the studies previously presented). Regarding this trend, some hypotheses are raised: (i) the LC<sup>3</sup> systems evaluated have a higher  $w/b$  ratio than those usually adopted for Portland cement

pastes, which may have contributed to the dispersion of CNT; (ii) the smaller particle size of the MK (see Table 2) aided in the CNT dispersion; (iii) the high reduction of the clinker factor in LC<sup>3</sup> systems alters the pH and the ionic concentration of the pore solution, also affecting the stability of the carboxyl functionalized CNT dispersion in this environment. Furthermore, in LC<sup>3</sup> systems, the negative charge of MK can adsorb high quantities of Ca<sup>2+</sup>, reducing its availability in the pore solution of the system [34], [56], [57]. Mendoza et al. [58] observed that alkaline environments with Ca(OH)<sub>2</sub> affect the stability of OH-functionalized CNT, increasing the agglomeration tendency of these nanomaterials. The CNT agglomeration occurs due to pH modification, the interaction among cations in the solution, and the negative surface charge of nanomaterial [23]. Thus, the lower pH [32], [59], [60] due to the high percentages of clinker replacement and the adsorption of Ca<sup>2+</sup> by calcined clays in LC<sup>3</sup> systems possibly contribute to reducing the tendency of CNT to agglomerate compared to Portland cement systems. However, a detailed investigation of the CNT dispersion in LC<sup>3</sup> pore solution should be carried out in future studies.

The hysteresis area (i.e., the area between the ascending and descending flow curves) of Portland cement-based materials can be associated with their thixotropic behaviour [61]. This behaviour is due to the colloidal flocculation and the early hydrates formation [62]. According to Hou et al. [63], the thixotropic behaviour of LC<sup>3</sup> is dominated by the flocculation of the system due to the negative surface charge and water affinity of calcined clay. In turn, for cementitious composites, the hysteresis area also can be related to the agglomeration of the nanomaterials [64]. Figure 4 shows the hysteresis area of CNT cementitious composites after 10 minutes of hydration. The hysteresis area values observed were of 29.7 Pa/s (REF), 157.1 Pa/s (0.05CNT), 116.0 Pa/s (0.075CNT), 126.2 Pa/s (0.1CNT), and 126.6 Pa/s (0.125CNT). There is an increase in the hysteresis area with the CNT incorporation compared to the plain cement paste (REF). Nevertheless, the increase in the CNT content did not result in a progressive increase in the hysteresis area of cement pastes. These results suggest that higher CNT contents can be incorporated into LC<sup>3</sup> systems. Note that the sonication parameters were fixed for all evaluated CNT contents. Thus, the increase in the nanomaterial content did not result in a higher agglomeration, as suggested by the hysteresis area results, even for the lower dispersion energy (J/g of CNT) applied for higher CNT contents. Nevertheless, in addition to the properties in the fresh state, the impact of higher CNT contents on hydration and mechanical properties of LC<sup>3</sup> systems also needs to be evaluated.

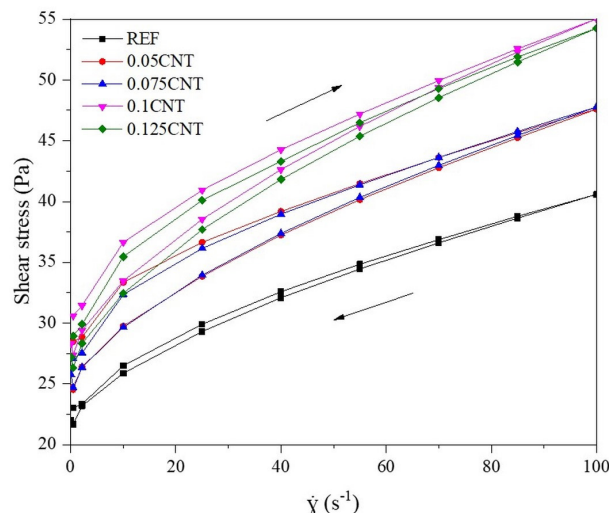


**Figure 4.** Ascending and descending flow curves of CNT cementitious composites after 10 minutes of hydration.

### 3.2 Hydration

Figure 5 shows the isothermal calorimetry curves of LC<sup>3</sup> pastes up to 120 hours, with normalized heat flow per gram of cement. The main peak of the silicate reaction is designated as “*Sp*”. It is mainly associated with the C<sub>3</sub>S (tricalcium silicate) hydration, while the consumption of sulfates is identified as “*SD*” and the peak of the aluminate reaction is denominated as “*Ap*”. All LC<sup>3</sup> with the CNT incorporation were properly sulfated since *Ap* occurred after *Sp* [65]. The reaction shows the four typical stages of PC hydration during the first 24 h of the pastes, being (1) dissolution, (2) induction, (3) acceleration, and (4) deceleration periods. The second stage corresponds to the induction period, followed by the acceleration period corresponding to the alite peak (Figure 5a), which occurs at 4-4.5

h for all LC<sup>3</sup> systems, with higher intensity for 0.05CNT (3.30 mW/g). During the induction period and the alite peak, part of the sulfate is consumed for ettringite precipitation, and part is adsorbed on C-S-H until the total depletion of sulfates in the system (Figure 5a) [66]. Therefore, the aluminate peak (Figure 5b) is related to ettringite formation from the reaction of C<sub>3</sub>A with the sulfate ions adsorbed on C-S-H [67]. The aluminate peak was higher for 0.075CNT (5.46 mW/g), which occurred at 7.86h, and for 0.1CNT (5.45 mW/g), occurring at 7.68h. The CNT incorporation provides the system with an additional surface area for contents up to 0.1, impacting the acceleration of sulfate consumption in LC<sup>3</sup> systems [68]. However, contents higher than 0.1 wt.%, there is a delay in the sulfate’s consumption and a lower heat flow at the peak of aluminates compared to the other CNT contents evaluated. Finally, Fig. 5c shows a “broad peak” at heat flow curves associated with the conversion of ettringite into AFm phases [69].

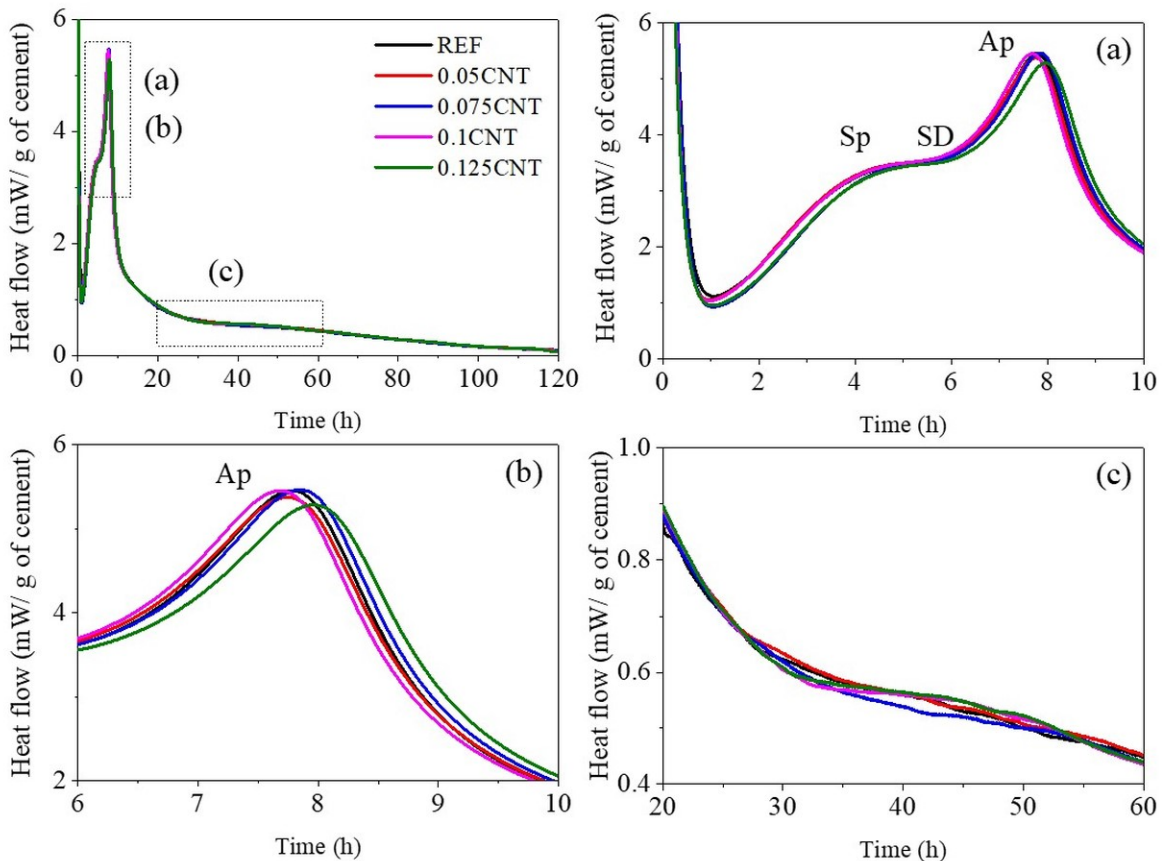


**Figure 5.** Heat flow of CNT cementitious composites and zoom of regions of interest (a,b and c) (Sp: silicate peak, Ap: aluminate peak, SD: sulfate depletion).

Generally, CNT accelerates cement hydration [70], [71]. However, some studies have indicated delays in PC hydration [72], [73], attributed to the CNT dispersion method and an inefficient dispersion. In this investigation, adding the different CNT contents did not cause significant curve changes. Only 0.125 CNT content was observed to promote a slight delay in the heat flow in the hydration process of the LC<sup>3</sup> systems. Stynoski et al. [74] also found no significant changes in hydration kinetics up to 35 hours. This can be explained due to the nanoparticles acting as a filler effect on the matrix [75].

The cumulative heat released after 120 hours was of 281.7 J/g (REF), 282.2 J/g (0.05CNT), 277.4 J/g (0.1CNT), 280.8 J/g (0.1CNT), and 280.4 J/g (0.125 CNT). This cumulative heat released by LC<sup>3</sup> systems with the incorporation of CNT is within the standard deviation range (7 J/g of cement) reported by Scrivener et al. [76], associated with the repeatability of the calorimetry test. These values indicate that CNTs did not significantly affect the hydration degree of LC<sup>3</sup> systems after 120 h.

### 3.3 Compressive strength

Figure 6 shows the average compressive strength values of the LC<sup>3</sup> systems at 7 and 28 days. Table S1 (<https://doi.org/10.48331/scielodata.YB6XVR>) summarizes the results of the statistical analysis (ANOVA) of these values. The two factors evaluated (CNT content and age) significantly influenced compressive strength. At 7 days, only 0.1CNT showed compressive strength gains of 13.5% compared to plain LC<sup>3</sup> (i.e., REF). This is consistent with the trend observed in the values of heat accumulated in the calorimetry. CNTs may have acted only through a physical effect of pore filling and matrix densification, not significantly altering the hydration kinetics. At 28 days, the increase in strength is more pronounced with CNT incorporation. The compressive strength of CNT-LC<sup>3</sup> composites reached values of 41-46 MPa. The optimal CNT contents were 0.075% and 0.1% by weight of cement, with gains of 9.6% and 13.2% compared to plain cement pastes, respectively. The explanation for this occurrence was previously discussed, and these incorporation contents are corroborated by some studies [19], [77], [78]. Furthermore, the compressive strength values of CNT-LC<sup>3</sup> composites reached the minimum mechanical requirements for Brazilian cement [79]. All CNT-LC<sup>3</sup> systems evaluated exhibited compressive strength values higher than CP IV-40 (Portland Pozzolan Cement) and CP V-ARI (Portland Cement of High Initial Strength), mainly at an early age.

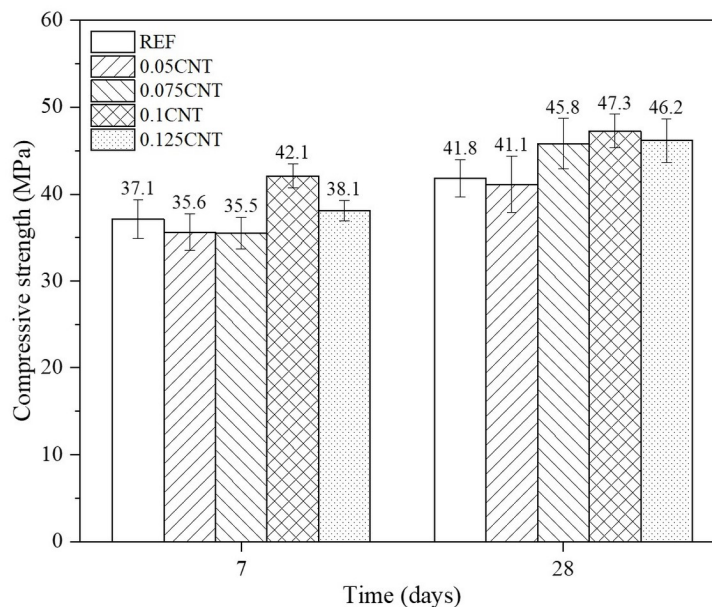


**Figure 6.** Compressive strength of CNT cementitious composites at 7 and 28 days of hydration. Error bars represent  $\pm 1$  standard deviation.

### 3.4 XRD

Figure 7 shows the selected ranges between  $7.5^{\circ} - 15^{\circ}$  (Figure 7a) and  $17^{\circ} - 20^{\circ}$  (Figure 7b)  $2\theta$  of XRD patterns of the CNT-LC<sup>3</sup> systems after 28 days of hydration. The crystalline peaks identified were: ettringite (COD 9011576), hemicarboaluminate (COD 2105252), monocarboaluminate (COD 2007668), and portlandite (COD 2101033). The presence of monosulfate was not identified. As previously reported, the limestone incorporation favours the hemicarboaluminate and monocarboaluminate formation instead of monosulfate [80]–[82]. After 28 days of hydration, the intensity of the ettringite and AFm phases peaks of CNT-LC<sup>3</sup> composites are generally similar, regardless of the CNT content. This behaviour can be attributed to the indirect stabilization of ettringite due to the formation of AFm phases, which leads to an increase in the hydrates volume and, therefore, a decrease in porosity, also explaining the compressive strength results previously discussed [82]. Similarly, the main portlandite peak at  $18.1^{\circ} 2\theta$  (Figure 7b) did not seem to be significantly modified by the incorporation of CNT, mainly considering that this peak can be affected by the preferential orientation of the crystals [19]. The XRD results are in line with the cumulative heat, which also indicated a similar hydration degree of CNT cementitious composites after 120 hours.

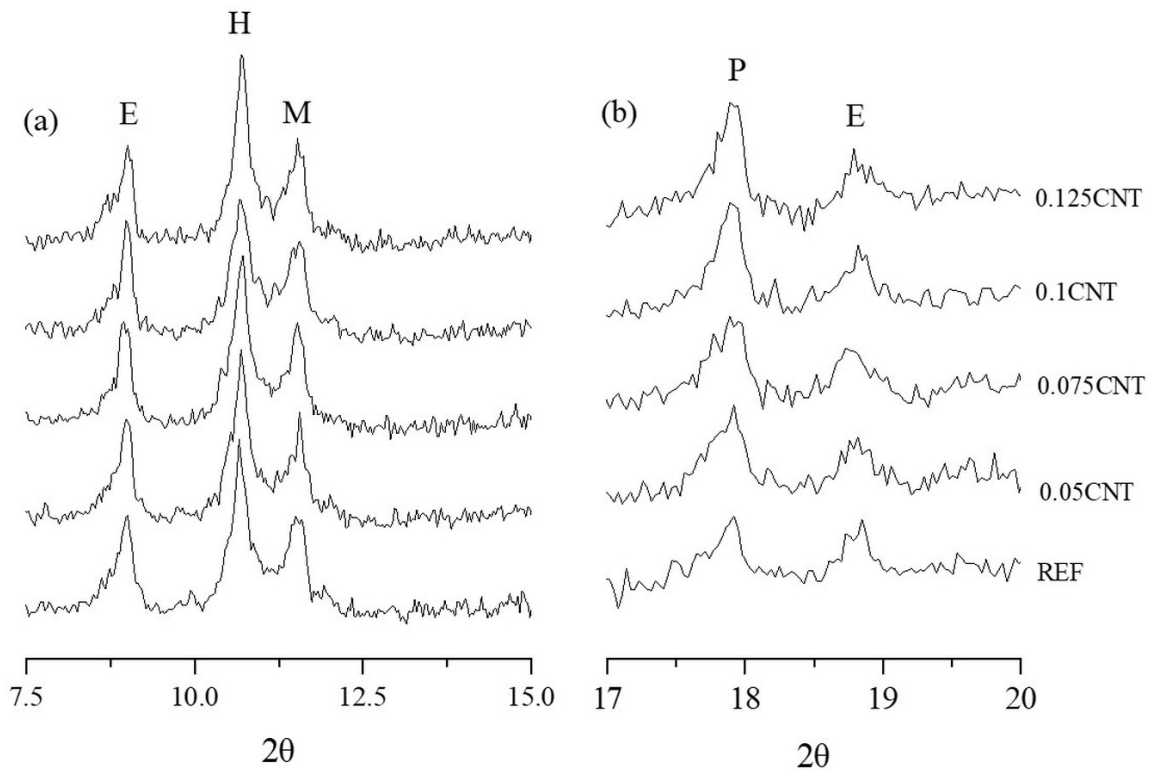


**Figure 7.** XRD patterns from  $7.5^{\circ}$  to  $15.0^{\circ}$  and  $17^{\circ}$  to  $20^{\circ}$   $2\theta$  of CNT cementitious composites at 28 days (E: ettringite; H: hemicarboaluminate, M: monocarboaluminate).

#### 4 CONCLUSIONS

The effect of CNT incorporation on the fresh and hardened-state properties of  $LC^3$  systems was assessed in this study. The following conclusions can be drawn:

- All  $LC^3$  compositions evaluated exhibited increased yield stress and viscosity during the first 60 minutes of hydration, mainly attributed to MK characteristics (e.g., high negative zeta potential, high specific surface area, and lower density). The CNT incorporation increased up to 25.7% and 65.0% on the dynamic yield stress and equivalent viscosity of  $LC^3$  cement pastes, respectively. Moreover, it is suggested to investigate further the impact of pH, and ionic environment of  $LC^3$  systems on the stability of CNT functionalized with the carboxyl/hydroxyl groups.
- The aluminate peak was slightly anticipated for a CNT content of 0.1 wt.% compared to the plain cement paste (REF). For higher CNT contents (e.g., 0.125 wt.%), a slight reduction in aluminates heat flow peak and a delay in the sulfate's consumption was observed. Regardless of the CNT content, the nanomaterial's incorporation did not significantly affect the 120h cumulative heat of cement pastes.
- A CNT content of 0.1 wt.% increased the compressive strength of  $LC^3$  by up to 13.5% and 13.2% for a hydration time of 7 and 28 days, respectively. The CNT effect on the mechanical properties is essentially attributed to a physical effect (e.g., pore filling).
- XRD results after 28 days of hydration showed that the CNT contents evaluated did not significantly modify the ettringite, AFm phases, and portlandite peaks intensity.

This research contributed to developing cement with lower  $CO_2$  emissions and CNT- $LC^3$  composites. Furthermore, a discussion on the dispersion of functionalized CNTs in  $LC^3$  systems is presented, bringing significant and relevant contributions to the study area. It is suggested that future studies analyze the impact of these nanomaterials on the mechanical properties and porosity of  $LC^3$  cementitious composites at early ages (e.g., 1 and 3 days).

#### ACKNOWLEDGEMENTS

The authors acknowledged the National Council for Scientific and Technological Development (CNPq), Coordination for the Improvement of Higher Education Personnel (CAPES), and Santa Catarina Research Foundation

(FAPESC). The authors also acknowledge the LDRX multi-user lab for the clinker XRD characterization. Esmalglass do Brazil is also acknowledged for donating the kaolin used in the study. L.S. acknowledged Intercement for financial support through the postdoctoral fellowship.

## REFERENCES

- [1] D. C. Reis, M. Quattrone, J. F. T. Souza, K. R. G. Punhagui, S. A. Pacca, and V. M. John, "Potential CO<sub>2</sub> reduction and uptake due to industrialization and efficient cement use in Brazil by 2050," *J. Ind. Ecol.*, vol. 25, pp. 344–358, 2021, <http://dx.doi.org/10.1111/jiec.13130>.
- [2] M. Sharma, S. Bishnoi, F. Martirena, and K. Scrivener, "Limestone calcined clay cement and concrete: a state-of-the-art review," *Cement Concr. Res.*, vol. 149, pp. 106564, 2021, <http://dx.doi.org/10.1016/j.cemconres.2021.106564>.
- [3] B. Wang, L. Yan, Q. Fu, and B. Kasal, "A comprehensive review on recycled aggregate and recycled aggregate concrete," *Resour. Conserv. Recycling*, vol. 171, pp. 105565, 2021, <http://dx.doi.org/10.1016/j.resconrec.2021.105565>.
- [4] United Nations Environment Programme, *Climate Ambition Alliance: Net Zero 2050*, Nairobi, Kenya: UNEP, 2020.
- [5] J. Rissman et al., "Technologies and policies to decarbonize global industry: review and assessment of mitigation drivers through 2070," *Appl. Energy*, vol. 266, pp. 114848, 2020, <http://dx.doi.org/10.1016/j.apenergy.2020.114848>.
- [6] S. Sánchez Berriel et al., "Assessing the environmental and economic potential of Limestone Calcined Clay Cement in Cuba," *J. Clean. Prod.*, vol. 124, pp. 361–369, 2016, <http://dx.doi.org/10.1016/j.jclepro.2016.02.125>.
- [7] L. M. Vizcaíno-Andrés, S. Sánchez-Berriel, S. Damas-Carrera, A. Pérez-Hernández, K. L. Scrivener, and J. F. Martirena-Hernández, "Industrial trial to produce a low clinker, low carbon cement," *Mater. Constr.*, vol. 65, pp. e045, 2015, <http://dx.doi.org/10.3989/mc.2015.00614>.
- [8] J. Yu, H. L. Wu, D. K. Mishra, G. Li, and C. K. Leung, "Compressive strength and environmental impact of sustainable blended cement with high-dosage Limestone and Calcined Clay (LC2)," *J. Clean. Prod.*, vol. 278, pp. 123616, 2021, <http://dx.doi.org/10.1016/j.jclepro.2020.123616>.
- [9] F. Avet, R. Snellings, A. Alujas Diaz, M. Ben Haha, and K. Scrivener, "Development of a new rapid, relevant and reliable (R3) test method to evaluate the pozzolanic reactivity of calcined kaolinitic clays," *Cement Concr. Res.*, vol. 85, pp. 1–11, 2016, <http://dx.doi.org/10.1016/j.cemconres.2016.02.015>.
- [10] K. Scrivener, F. Martirena, S. Bishnoi, and S. Maity, "Calcined clay limestone cements (LC3)," *Cement Concr. Res.*, vol. 114, pp. 49–56, 2018, <http://dx.doi.org/10.1016/j.cemconres.2017.08.017>.
- [11] F.H. Avet, "Investigation of the grade of calcined clays used as clinker substitute in Limestone Calcined Clay Cement (LC3)," Ph.D. dissertation, École Polytech. Féd. Lausanne, Suisse, FR, 2017.
- [12] J. J. Biernacki et al., "Cements in the 21 st century: challenges, perspectives, and opportunities," *J. Am. Ceram. Soc.*, vol. 100, pp. 2746–2773, 2017, <http://dx.doi.org/10.1111/jace.14948>.
- [13] B. Sabir, S. Wild, and J. Bai, "Metakaolin and calcined clays as pozzolans for concrete: A review," *Cement Concr. Compos.*, vol. 23, pp. 441–454, 2001, [http://dx.doi.org/10.1016/S0958-9465\(00\)00092-5](http://dx.doi.org/10.1016/S0958-9465(00)00092-5).
- [14] T. R. Muzenda, P. Hou, S. Kawashima, T. Sui, and X. Cheng, "The role of limestone and calcined clay on the rheological properties of LC3," *Cement Concr. Compos.*, vol. 107, pp. 103516, 2020, <http://dx.doi.org/10.1016/j.cemconcomp.2020.103516>.
- [15] S. Ferreira, D. Herfort, and J. S. Damtoft, "Effect of raw clay type, fineness, water-to-cement ratio and fly ash addition on workability and strength performance of calcined clay – Limestone Portland cements," *Cement Concr. Res.*, vol. 101, pp. 1–12, 2017, <http://dx.doi.org/10.1016/j.cemconres.2017.08.003>.
- [16] A. Cuesta, A. Morales-Cantero, A. G. De la Torre, and M. A. G. Aranda, "Recent advances in C-S-H nucleation seeding for improving cement performances," *Materials (Basel)*, vol. 16, 2023, <http://dx.doi.org/10.3390/ma16041462>.
- [17] D. Y. Yoo, I. You, and S. J. Lee, "Electrical and piezoresistive sensing capacities of cement paste with multi-walled carbon nanotubes," *Arch. Civ. Mech. Eng.*, vol. 18, pp. 371–384, 2018, <http://dx.doi.org/10.1016/j.acme.2017.09.007>.
- [18] A. Sobolkina et al., "Dispersion of carbon nanotubes and its influence on the mechanical properties of the cement matrix," *Cement Concr. Compos.*, vol. 34, pp. 1104–1113, 2012, <http://dx.doi.org/10.1016/j.cemconcomp.2012.07.008>.
- [19] J. S. Andrade No., T. A. Santos, S. A. Pinto, C. M. R. Dias, and D. V. Ribeiro, "Effect of the combined use of carbon nanotubes (CNT) and metakaolin on the properties of cementitious matrices," *Constr. Build. Mater.*, vol. 271, 2021, <http://dx.doi.org/10.1016/j.conbuildmat.2020.121903>.
- [20] L. Silvestro et al., "Influence of ultrasonication of functionalized carbon nanotubes on the rheology, hydration, and compressive strength of portland cement pastes," *Materials (Basel)*, vol. 14, pp. 5248, 2021, <http://dx.doi.org/10.3390/ma14185248>.
- [21] S. K. Adhikary, Ž. Rudžionis, S. Tučkutė, and D. K. Ashish, "Effects of carbon nanotubes on expanded glass and silica aerogel based lightweight concrete," *Sci. Rep.*, vol. 11, pp. 1–11, 2021, <http://dx.doi.org/10.1038/s41598-021-81665-y>.

- [22] L. Silvestro and P. J. P. Gleize, "Effect of carbon nanotubes on compressive, flexural and tensile strengths of Portland cement-based materials : a systematic literature review," *Constr. Build. Mater.*, vol. 264, pp. 120237, 2020, <http://dx.doi.org/10.1016/j.conbuildmat.2020.120237>.
- [23] O. A. M. Reales and R. D. Toledo Fo., "A review on the chemical, mechanical and microstructural characterization of carbon nanotubes-cement based composites," *Constr. Build. Mater.*, vol. 154, pp. 697–710, 2017, <http://dx.doi.org/10.1016/j.conbuildmat.2017.07.232>.
- [24] K. M. Liew, M. F. Kai, and L. W. Zhang, "Carbon nanotube reinforced cementitious composites: An overview," *Compos., Part A Appl. Sci. Manuf.*, vol. 91, pp. 301–323, 2016, <http://dx.doi.org/10.1016/j.compositesa.2016.10.020>.
- [25] F. Naeem, H. K. Lee, H. K. Kim, and I. W. Nam, "Flexural stress and crack sensing capabilities of MWNT/cement composites," *Compos. Struct.*, vol. 175, pp. 86–100, 2017, <http://dx.doi.org/10.1016/j.compstruct.2017.04.078>.
- [26] H. A. Gamal, M. S. El-Feky, Y. R. Alharbi, A. A. Abadel, and M. Kohail, "Enhancement of the concrete durability with hybrid nano materials," *Sustain.*, vol. 13, pp. 1–17, 2021, <http://dx.doi.org/10.3390/su13031373>.
- [27] M. S. Morsy, S. H. Alsayed, and M. Aqel, "Hybrid effect of carbon nanotube and nano-clay on physico-mechanical properties of cement mortar," *Constr. Build. Mater.*, vol. 25, pp. 145–149, 2011, <http://dx.doi.org/10.1016/j.conbuildmat.2010.06.046>.
- [28] S. Ma, Y. Qian, and S. Kawashima, "Performance-based study on the rheological and hardened properties of blended cement mortars incorporating palygorskite clays and carbon nanotubes," *Constr. Build. Mater.*, vol. 171, pp. 663–671, 2018, <http://dx.doi.org/10.1016/j.conbuildmat.2018.03.121>.
- [29] R. S. Lin, S. Oh, W. Du, and X. Y. Wang, "Strengthening the performance of limestone-calcined clay cement (LC3) using nano silica," *Constr. Build. Mater.*, vol. 340, pp. 127723, 2022, <http://dx.doi.org/10.1016/j.conbuildmat.2022.127723>.
- [30] C. S. Malacarne, M. A. Longhi, M. R. C. Silva, J. P. Gonçalves, E. D. Rodríguez, and A. P. Kirchheim, "Influence of low-grade materials as clinker substitute on the rheological behavior, hydration and mechanical performance of ternary cements," *Case Stud. Constr. Mater.*, vol. 15, pp. e00776, 2021, <http://dx.doi.org/10.1016/j.cscm.2021.e00776>.
- [31] M. Antoni, J. Rossen, F. Martirena, and K. Scrivener, "Cement substitution by a combination of metakaolin and limestone," *Cement Concr. Res.*, vol. 42, pp. 1579–1589, 2012, <http://dx.doi.org/10.1016/j.cemconres.2012.09.006>.
- [32] F. Zunino and K. Scrivener, "The reaction between metakaolin and limestone and its effect in porosity refinement and mechanical properties," *Cement Concr. Res.*, vol. 140, pp. 106307, 2021, <http://dx.doi.org/10.1016/j.cemconres.2020.106307>.
- [33] R. Sposito, M. Maier, N. Beuntner, and K. C. Thienel, "Evaluation of zeta potential of calcined clays and time-dependent flowability of blended cements with customized polycarboxylate-based superplasticizers," *Constr. Build. Mater.*, vol. 308, pp. 125061, 2021, <http://dx.doi.org/10.1016/j.conbuildmat.2021.125061>.
- [34] M. Schmid and J. Plank, "Interaction of individual meta clays with polycarboxylate (PCE) superplasticizers in cement investigated via dispersion, zeta potential and sorption measurements," *Appl. Clay Sci.*, vol. 207, 2021, <http://dx.doi.org/10.1016/j.clay.2021.106092>.
- [35] W. Zhang et al., "Influence of acid-treated time of carbon nanotubes on mechanical property in carbon nanotubes reinforced copper matrix composites," *Diamond Related Materials*, vol. 109, pp. 108069, 2020, <http://dx.doi.org/10.1016/j.diamond.2020.108069>.
- [36] J. Kathi, K. Y. Rhee, and J. H. Lee, "Effect of chemical functionalization of multi-walled carbon nanotubes with 3-aminopropyltriethoxysilane on mechanical and morphological properties of epoxy nanocomposites," *Compos., Part A Appl. Sci. Manuf.*, vol. 40, pp. 800–809, 2009, <http://dx.doi.org/10.1016/j.compositesa.2009.04.001>.
- [37] T. C. Cardoso, P. R. de Matos, L. Py, M. Longhi, O. Cascudo, and A. P. Kirchheim, "Ternary cements produced with non-calcined clay, limestone, and Portland clinker," *J. Build. Eng.*, vol. 45, pp. 103437, 2022, <http://dx.doi.org/10.1016/j.jobbe.2021.103437>.
- [38] J. E. L. de Siqueira and P. J. P. Gleize, "Effect of carbon nanotubes sonication on mechanical properties of cement pastes," *Rev. IBRACON Estrut. Mater.*, vol. 13, pp. 455–463, 2020, <http://dx.doi.org/10.1590/s1983-41952020000200013>.
- [39] L. Silvestro, A. Spat Ruviaro, P. Ricardo de Matos, F. Pelisser, D. Zambelli Mezalira, and P. Jean Paul Gleize, "Functionalization of multi-walled carbon nanotubes with 3-aminopropyltriethoxysilane for application in cementitious matrix," *Constr. Build. Mater.*, vol. 311, pp. 125358, 2021, <http://dx.doi.org/10.1016/j.conbuildmat.2021.125358>.
- [40] L. Silvestro, G. T. dos Santos Lima, A. S. Ruviaro, P. R. de Matos, D. Z. Mezalira, and P. J. P. Gleize, "Evaluation of different organosilanes on multi-walled carbon nanotubes functionalization for application in cementitious composites," *J. Build. Eng.*, vol. 51, pp. 104292, 2022, <http://dx.doi.org/10.1016/j.jobbe.2022.104292>.
- [41] O. H. Wallevik, D. Feys, J. E. Wallevik, and K. H. Khayat, "Avoiding inaccurate interpretations of rheological measurements for cement-based materials," *Cement Concr. Res.*, vol. 78, pp. 100–109, 2015, <http://dx.doi.org/10.1016/j.cemconres.2015.05.003>.
- [42] F. De Larrard, C. F. Ferraris, and T. Sedran, "Fresh concrete: a Herschel-Bulkley material," *Mater. Struct. Constr.*, vol. 31, pp. 494–498, 1996, <http://dx.doi.org/10.1007/bf02480474>.
- [43] D. L. Kantro, "Influence of water-reducing admixtures on properties of cement paste - a miniature slump test," *Cem. Concr. Aggregates*, vol. 2, pp. 95–102, 1980. <https://doi.org/http://dx.doi.org/10.1520/CCA10190J>.
- [44] R. Sposito, N. Beuntner, and K. C. Thienel, "Rheology, setting and hydration of calcined clay blended cements in interaction with PCE-based superplasticisers," *Mag. Concr. Res.*, vol. 73, pp. 785–797, 2021, <http://dx.doi.org/10.1680/jmacr.19.00488>.

- [45] R. Sposito, N. Beuntner, and K. C. Thienel, "Characteristics of components in calcined clays and their influence on the efficiency of superplasticizers," *Cement Concr. Compos.*, vol. 110, 2020, <http://dx.doi.org/10.1016/j.cemconcomp.2020.103594>.
- [46] C. Jakob et al., "Relating ettringite formation and rheological changes during the initial cement hydration: a comparative study applying XRD analysis, rheological measurements and modeling," *Materials (Basel)*, vol. 12, no. 18, pp. 2957, 2019, <http://dx.doi.org/10.3390/ma12182957>.
- [47] I. Navarrete, Y. Kurama, N. Escalona, W. Brevis, and M. Lopez, "Effect of supplementary cementitious materials on viscosity of cement-based pastes," *Cement Concr. Res.*, vol. 151, pp. 106635, 2022, <http://dx.doi.org/10.1016/j.cemconres.2021.106635>.
- [48] N. Roussel, *Understanding the Rheology of Concrete*, Cambridge: Woodhead Publishing, 2011. <https://doi.org/10.1533/9780857095282>.
- [49] N. Roussel, "Rheology of fresh concrete: from measurements to predictions of casting processes," *Mater. Struct. Constr.*, vol. 40, pp. 1001–1012, 2007, <http://dx.doi.org/10.1617/s11527-007-9313-2>.
- [50] S. Jiang et al., "Rheological properties of cementitious composites with nano/fiber fillers," *Constr. Build. Mater.*, vol. 158, pp. 786–800, 2018, <http://dx.doi.org/10.1016/j.conbuildmat.2017.10.072>.
- [51] O. A. M. Reales, P. Duda, and R. D. Filho, "Effect of a carbon nanotube/surfactant aqueous dispersion on the rheological and mechanical properties of portland cement pastes," *J. Mater. Civ. Eng.*, vol. 30, pp. 1–8, 2018, [http://dx.doi.org/10.1061/\(ASCE\)MT.1943-5533.0002452](http://dx.doi.org/10.1061/(ASCE)MT.1943-5533.0002452).
- [52] F. De Larrard and T. Sedran, "Mixture-proportioning of high-performance concrete," *Cement Concr. Res.*, vol. 32, pp. 1699–1704, 2002, [http://dx.doi.org/10.1016/S0008-8846\(02\)00861-X](http://dx.doi.org/10.1016/S0008-8846(02)00861-X).
- [53] O. A. M. Reales, Y. P. Arias Jaramillo, J. C. Ochoa Botero, C. A. Delgado, J. H. Quintero, and R. D. Toledo Filho, "Influence of MWCNT/surfactant dispersions on the rheology of Portland cement pastes," *Cement Concr. Res.*, vol. 107, pp. 101–109, 2018, <http://dx.doi.org/10.1016/j.cemconres.2018.02.020>.
- [54] S. Musso, J. M. Tulliani, G. Ferro, and A. Tagliaferro, "Influence of carbon nanotubes structure on the mechanical behavior of cement composites," *Compos. Sci. Technol.*, vol. 69, pp. 1985–1990, 2009, <http://dx.doi.org/10.1016/j.compscitech.2009.05.002>.
- [55] Z. Li, D. J. Corr, B. Han, and S. P. Shah, "Investigating the effect of carbon nanotube on early age hydration of cementitious composites with isothermal calorimetry and Fourier transform infrared spectroscopy," *Cement Concr. Compos.*, vol. 107, pp. 103513, 2020, <http://dx.doi.org/10.1016/j.cemconcomp.2020.103513>.
- [56] R. Li, L. Lei, T. Sui, and J. Plank, "Effectiveness of PCE superplasticizers in calcined clay blended cements," *Cement Concr. Res.*, vol. 141, pp. 106334, 2021, <http://dx.doi.org/10.1016/j.cemconres.2020.106334>.
- [57] M. Maier, R. Sposito, N. Beuntner, and K. C. Thienel, "Particle characteristics of calcined clays and limestone and their impact on early hydration and sulfate demand of blended cement," *Cement Concr. Res.*, vol. 154, pp. 106736, 2022., <http://dx.doi.org/10.1016/j.cemconres.2022.106736>.
- [58] O. Mendoza, G. Sierra, and J. I. Tobón, "Influence of super plasticizer and Ca(OH)<sub>2</sub> on the stability of functionalized multi-walled carbon nanotubes dispersions for cement composites applications," *Constr. Build. Mater.*, vol. 47, pp. 771–778, 2013, <http://dx.doi.org/10.1016/j.conbuildmat.2013.05.100>.
- [59] F. Avet, L. Sofia, and K. Scrivener, "Concrete performance of limestone calcined clay cement (LC3) compared with conventional cements," *Adv. Civ. Eng. Mater.*, vol. 8, pp. 275–286, 2019, <http://dx.doi.org/10.1520/ACEM20190052>.
- [60] F. Avet and K. Scrivener, "Influence of pH on the chloride binding capacity of Limestone Calcined Clay Cements (LC3)," *Cement Concr. Res.*, vol. 131, pp. 106031, 2020, <http://dx.doi.org/10.1016/j.cemconres.2020.106031>.
- [61] D. Jiao, C. Shi, and Q. Yuan, "Influences of shear-mixing rate and fly ash on rheological behavior of cement pastes under continuous mixing," *Constr. Build. Mater.*, vol. 188, pp. 170–177, 2018, <http://dx.doi.org/10.1016/j.conbuildmat.2018.08.091>.
- [62] N. Roussel, G. Ovarlez, S. Garrault, and C. Brumaud, "The origins of thixotropy of fresh cement pastes," *Cement Concr. Res.*, vol. 42, pp. 148–157, 2012, <http://dx.doi.org/10.1016/j.cemconres.2011.09.004>.
- [63] P. Hou et al., "Mechanisms dominating thixotropy in limestone calcined clay cement (LC3)," *Cement Concr. Res.*, vol. 140, pp. 106316, 2021, <http://dx.doi.org/10.1016/j.cemconres.2020.106316>.
- [64] O. A. M. Reales, P. Duda, and R. Dias Toledo Fo., "Effect of a carbon nanotube/surfactant aqueous dispersion on the rheological and mechanical properties of Portland Cement Pastes," *J. Mater. Civ. Eng.*, vol. 30, pp. 04018259, 2018., [http://dx.doi.org/10.1061/\(asce\)mt.1943-5533.0002452](http://dx.doi.org/10.1061/(asce)mt.1943-5533.0002452).
- [65] J. S. Andrade No., A. G. De la Torre, A. P. Kirchheim, "Effects of sulfates on the hydration of Portland cement – A review," *Constr. Build. Mater.*, vol. 279, 2021, <http://dx.doi.org/10.1016/j.conbuildmat.2021.122428>.
- [66] A. Quennoz and K. L. Scrivener, "Interactions between alite and C3A-gypsum hydrations in model cements," *Cement Concr. Res.*, vol. 44, pp. 46–54, 2013, <http://dx.doi.org/10.1016/j.cemconres.2012.10.018>.
- [67] K. L. Scrivener, P. Juilland, and P. J. M. Monteiro, "Advances in understanding hydration of Portland cement," *Cement Concr. Res.*, vol. 78, pp. 38–56, 2015, <http://dx.doi.org/10.1016/j.cemconres.2015.05.025>.

- [68] S. Aodkeng, S. Sinthupinyo, B. Chamnankid, W. Hanpongpun, and A. Chaipanich, "Effect of carbon nanotubes/clay hybrid composite on mechanical properties, hydration heat and thermal analysis of cement-based materials," *Constr. Build. Mater.*, vol. 320, pp. 126212, 2022, <http://dx.doi.org/10.1016/j.conbuildmat.2021.126212>.
- [69] J. W. Bullard et al., "Mechanisms of cement hydration," *Cement Concr. Res.*, vol. 41, pp. 1208–1223, 2011., <http://dx.doi.org/10.1016/j.cemconres.2010.09.011>.
- [70] R. Nadiv, M. Shtein, M. Refaeli, A. Peled, and O. Regev, "The critical role of nanotube shape in cement composites," *Cement Concr. Compos.*, vol. 71, pp. 166–174, 2016, <http://dx.doi.org/10.1016/j.cemconcomp.2016.05.012>.
- [71] B. Wang and B. Pang, "Properties improvement of multiwall carbon nanotubes-reinforced cement-based composites," *J. Compos. Mater.*, vol. 54, pp. 2379–2387, 2020, <http://dx.doi.org/10.1177/0021998319896835>.
- [72] P. Sikora, M. Abd Elrahman, S. Y. Chung, K. Cendrowski, E. Mijowska, and D. Stephan, "Mechanical and microstructural properties of cement pastes containing carbon nanotubes and carbon nanotube-silica core-shell structures, exposed to elevated temperature," *Cement Concr. Compos.*, vol. 95, pp. 193–204, 2019, <http://dx.doi.org/10.1016/j.cemconcomp.2018.11.006>.
- [73] O. A. Mendoza Reales, W. C. Pearl, M. D. M. Paiva, C. R. Miranda, and R. D. Toledo Filho, "Effect of a commercial dispersion of multi walled carbon nanotubes on the hydration of an oil well cementing paste," *Front. Struct. Civ. Eng.*, vol. 10, pp. 174–179, 2016, <http://dx.doi.org/10.1007/s11709-015-0324-8>.
- [74] P. Stynoski, P. Mondal, and C. Marsh, "Effects of silica additives on fracture properties of carbon nanotube and carbon fiber reinforced Portland cement mortar," *Cement Concr. Compos.*, vol. 55, pp. 232–240, 2015, <http://dx.doi.org/10.1016/j.cemconcomp.2014.08.005>.
- [75] H. Li, J. Ou, H. Xiao, X. Guan, and B. Han, "Nanomaterials-enabled multifunctional concrete and structures," in: *Nanotechnology in Civil Infrastructure*, K. Gopalakrishnan, B. Birgisson, P. Taylor and N.O. Attoh-Okine, Eds., Berlin, Heidelberg: Springer, 2011, pp. 131-173. [https://dx.doi.org/10.1007/978-3-642-16657-0\\_5](https://dx.doi.org/10.1007/978-3-642-16657-0_5).
- [76] K. Scrivener, R. Snellings, B. Lothenbach, *A Practical Guide to Microstructural Analysis of Cementitious Materials*, Boca Raton: CRC Press, 2018. <https://dx.doi.org/10.1201/b19074>.
- [77] T. Nochaiya and A. Chaipanich, "Behavior of multi-walled carbon nanotubes on the porosity and microstructure of cement-based materials," *Appl. Surf. Sci.*, vol. 257, pp. 1941–1945, 2011, <http://dx.doi.org/10.1016/j.apsusc.2010.09.030>.
- [78] F. Gao, W. Tian, Z. Wang, and F. Wang, "Effect of diameter of multi-walled carbon nanotubes on mechanical properties and microstructure of the cement-based materials," *Constr. Build. Mater.*, vol. 260, pp. 120452, 2020, <http://dx.doi.org/10.1016/j.conbuildmat.2020.120452>.
- [79] Associação Brasileira de Normas Técnicas, *Cimento Portland – Requisitos*, NBR 16697, 2018.
- [80] G. Cardinaud et al., "Calcined clay – Limestone cements: hydration processes with high and low-grade kaolinite clays," *Constr. Build. Mater.*, vol. 277, pp. 122271, 2021, <http://dx.doi.org/10.1016/j.conbuildmat.2021.122271>.
- [81] A. S. Ruviaro, L. Silvestro, T. P. Scolaro, P. R. de Matos, and F. Pelisser, "Use of calcined water treatment plant sludge for sustainable cementitious composites production," *J. Clean. Prod.*, 2021, <http://dx.doi.org/10.1016/j.jclepro.2021.129484>.
- [82] B. Lothenbach, G. Le Saout, E. Gallucci, and K. Scrivener, "Influence of limestone on the hydration of Portland cements," *Cement Concr. Res.*, vol. 38, pp. 848–860, 2008, <http://dx.doi.org/10.1016/j.cemconres.2008.01.002>.

## Supplementary Material

Supplementary material accompanies this paper.

Figure S1. XRD pattern of limestone filler.

Figure S2. XRD patterns of in natura kaolin and thermally activated metakaolin at 600, 700, 800, and 900 °C.

Figure S3. R<sup>3</sup> test results of in natura kaolin and thermally activated metakaolin at 600, 700, 800, and 900 °C.

Figure S4. Zeta potential of in natura kaolin and thermally activated metakaolin at 600, 700, 800, and 900 °C.

Table S1. ANOVA of compressive strength results.

This material is available from <https://doi.org/10.48331/scielodata.YB6XVR>

---

**Author contributions:** LS: conceptualization, data curation, formal analysis, investigation, methodology; ASR: conceptualization, data curation, formal analysis, investigation, methodology; FRRC: conceptualization, data curation, formal analysis, investigation, methodology, submission; PJPG: supervision, writing, revising; APK: supervision, revising, formal analysis.

**Editors:** Yury Villagrán Zaccardi, Guilherme Aris Parsekian.